β-Amyloid Precursor Protein Intracellular Domain Controls Mitochondrial Function by Modulating Phosphatase and Tensin Homolog–Induced Kinase 1 Transcription in Cells and in Alzheimer Mice Models

Thomas Goiran, Eric Duplan, Mounia Chami, Alexandre Bourgeois, Wejdane El Manaa, Lila Rouland, Julie Dunys, Inger Lauritzen, Han You, Vuk Stambolic, et al.

Archival Report

Biological Psychiatry

β-Amyloid Precursor Protein Intracellular Domain Controls Mitochondrial Function by Modulating Phosphatase and Tensin Homolog–Induced Kinase 1 Transcription in Cells and in Alzheimer Mice Models

Thomas Goiran, Eric Duplan, Mounia Chami, Alexandre Bourgeois, Wejdane El Manaa, Lila Rouland, Julie Dunys, Inger Lauritzen, Han You, Vuk Stambolic, Maria-Grazia Biféri, Martine Barkats, Sanjay W. Pimplikar, Nicolas Sergeant, Morvane Colin, Vanessa A. Morais, Raphaelle Pardossi-Piquard, Frédéric Checler, and Cristine Alves da Costa

ABSTRACT

BACKGROUND: Mitophagy and mitochondrial dynamics alterations are two major hallmarks of neurodegenerative diseases. Dysfunctional mitochondria accumulate in Alzheimer's disease–affected brains by yet unexplained mechanisms.

METHODS: We combined cell biology, molecular biology, and pharmacological approaches to unravel a novel molecular pathway by which presenilins control phosphatase and tensin homolog–induced kinase 1 (Pink-1) expression and transcription. In vivo approaches were carried out on various transgenic and knockout animals as well as in adeno-associated virus–infected mice. Functional readout and mitochondrial physiology (mitochondrial potential) were assessed by combined procedures including flow cytometry, live imaging analysis, and immunohistochemistry.

RESULTS: We show that presenilins 1 and 2 trigger opposite effects on promoter transactivation, messenger RNA, and protein expression of Pink-1. This control is linked to γ-secretase activity and β-amyloid precursor protein but is independent of phosphatase and tensin homolog. We show that amyloid precursor protein intracellular domain (AICD) accounts for presenilin-dependent phenotype and upregulates Pink-1 transactivation in cells as well as in vivo in a Forkhead box O3a–dependent manner. Interestingly, the modulation of γ-secretase activity or AICD expression affects Pink-1–related control of mitophagy and mitochondrial dynamics. Finally, we show that parkin acts upstream of presenilins to control Pink-1 promoter transactivation and protein expression.

CONCLUSIONS: Overall, we delineate a molecular cascade presenilins–AICD–Forkhead box O3a linking parkin to Pink-1. Our study demonstrates AICD-mediated Pink-1–dependent control of mitochondrial physiology by presenilins. Furthermore, it unravels a parkin–Pink-1 feedback loop controlling mitochondrial physiology that could be disrupted in neurodegenerative conditions.

Keywords: AICD, FOXO3a, γ-Secretase, Mitochondrial dysfunction, Mitophagy, Parkin, Pink-1, Presenilins, 3xTgAD Mice

http://dx.doi.org/10.1016/j.biopsych.2017.04.011

It arose recently that besides macroscopic lesions characterizing specific subsets of neurodegenerative diseases, mitochondrial function appears to be consistently affected in brain diseases (1,2). Indeed, mitochondrial deficits are now considered as a major hallmark in Alzheimer's disease (AD) (3). In both familial and sporadic AD cases, early accumulation of structurally abnormal mitochondria has been evidenced (4,5), and such defects also stand in animal models of AD (6). Thus, β-amyloid precursor protein (βAPP) transgenic mice-derived neurons display drastically altered mitochondrial dynamics (6,7).

Exacerbated neuronal autophagy/mitophagy also corresponds to a consistent anatomical stigma in neurodegenerative diseases (2). In AD-affected brains, electron microscopy unraveled neuronal accumulation of autophagic vacuoles and impairment of autophagosomes maturation that ultimately yield amyloid-β (Aβ) overload (8). While both mitochondrial dynamics and mitophagy could well contribute to early phase of AD-linked neurodegeneration, little is known concerning the mechanistic defects that could account for such alterations.

ISSN: 0006-3223

Phosphatase and tensin homolog (PTEN)-induced kinase 1 (Pink-1) controls both mitochondrial dynamics and mitophagy by selectively enhancing mitochondrial fission (9) and recruiting parkin (PK) to damaged mitochondria (10), respectively. Pink-1 is a PTEN-induced putative kinase 1 (11), and it is noteworthy that PTEN expression is altered in AD brains in a region-specific manner (12) and appears to be involved in the synaptic plasticity and cognition in AD mice models (13). Strikingly, immunological detection also revealed Pink-1 expression in senile plaques (14). Overall, alteration of PTEN-Pink-1 homeostasis could well account for some of the defects taking place in AD.

It is remarkable that presenilin 1 (PS1) and presenilin 2 (PS2), which constitute the catalytic core of γ-secretase responsible for the ultimate cleavage yielding Aβ (15,16) and its C-terminal counterpart APP intracellular domain (AICD) (17) from βAPP, regulate the level of PTEN (18). This led us to question of whether PSs could act as upstream regulators of Pink-1 and its associated functions. Here, we show that PS1 controls Pink-1 by a γ-secretase–dependent and βAPP-dependent but PTEN-independent mechanism. We show that AICD, which was shown to behave as a transcription factor (19–21), indeed controls Pink-1 transactivation and expression in a Forkhead box O3a (FOXO3a)-dependent process. AICD-mediated control of Pink-1 influences its mitochondrial and mitophagic functions. Finally, we demonstrate that PK, which acts as a transactivator of PS1 promoter (22), controls Pink-1 in a fully PS1-dependent but PTEN-independent manner. Thus, our study delineates, for the first time, a molecular cascade linking PS1 and Pink-1. Furthermore, we reveal a PS-dependent molecular link between PK and Pink-1 that could be part of a feedback loop responsible for their cellular homeostasis and mitochondrial health that could be altered in neurodegenerative condition.

METHODS AND MATERIALS

Cellular and animal models, promoter activities assay, messenger RNA (mRNA) analysis, and description of constructs are provided in the Supplement.

Drug Description and Administration Ex Vivo

The mitochondrial uncoupler carbonyl cyanide *m*-chlorophenyl hydrazone (CCCP) and LY294002 (2-(4-morpholinyl)-8-phenyl-1(4*H*)-benzopyran-4-one hydrochloride) (23) (Millipore-Sigma; St Quentin Fallavier, France) were incubated at 10 μM for 6 and 16 hours, respectively, as previously described (24). DFK-167 (MP Biomedical, Santa Ana, CA) was applied on human embryonic kidney 293 (HEK293) and mouse embryonic fibroblast cells at 50 μM for 15 hours. ELND006 (D6) was kindly provided by Elan Pharmaceuticals (South San Francisco, CA) and used in both ex vivo and in vivo studies (see "3xTgAD and In Vivo Drug Treatment" section below) (25). In ex vivo experiences, HEK293 and mouse embryonic fibroblast cells were treated for 15 hours with D6 (5 μM).

Cellular and Mouse Brain Sample Preparation and Western Blot Analysis

Western blot analysis of cellular and mouse brain samples was performed by standard procedures and is described in the Supplement.

3xTgAD Mice and In Vivo Drug Treatment

3xTgAD mice (harboring $PS1_{M146V}$, βAPP_{swe}, and TAU_{P301L} transgenes) and nontransgenic (wild-type) mice (26) were housed with a 12-hour light/dark cycle and were given free access to food and water. All experimental procedures were conducted in accordance with the European Communities Council Directive of November 24, 1986 (86/609/EEC) and local French legislation. Two groups of 24 wild-type male mice (129/C57BL/6) and 25 3xTgAD male mice were used. Mice were treated daily for 10 days with either vehicle or D6 (30 mg/kg) (Elan Pharmaceuticals) (25) via oral gavage (27). Animals were sacrificed 6 hours after the last administration. Dissected hippocampi were either submerged for 2 days in RNA*later* RNA Stabilization Reagent (Qiagen, Marseille, France) for quantitative polymerase chain reaction mRNA analysis or reserved for membrane fractions preparation devoted to γ-secretase activity measurement (28), and Western blot analysis of AICD and βAPP C-terminal fragments were performed as described in the Supplement.

Adeno-associated Virus-Nuclear Localization Sequence-AICD Production and Mice Injection

Virus production and mice injection were performed according to previously described protocols (27,29) and are resumed in the Supplement.

Mitochondrial Potential Disruption Analysis

Mitochondrial potential was accessed using live imaging and flow cytometry analysis of tetramethyl-rhodamine methyl ester probe as detailed in the Supplement.

Immunohistochemistry

Immunohistochemical analyses of mouse brain slices are described in the Supplement.

RESULTS

PS1 and PS2 Differently Modulate Pink-1 Transcription in a PTEN-Independent Manner

We have examined the ability of PS1 and PS2 to modulate Pink-1 levels at both transcriptional and posttranscriptional levels. We show that Pink-1 expression is poorly detectable in mock-transfected HEK293 cells and could be enhanced on CCCP treatment (Figure 1A, B), in agreement with the well-established stabilizing effect of this uncoupling agent on Pink-1 protein (10). Stable expression of PS1 drastically enhances Pink-1 expression, while PS2 reduces Pink-1 to levels below CCCP-treated mock-transfected cells (Figure 1A, B). Interestingly, PS1 and PS2 also trigger similar opposite effects on Pink-1 promoter transactivation (Figure 1C) and mRNA levels (Figure 1D).

PSs regulate cellular levels of PTEN (18), a tumor suppressor thought to transcriptionally transactivate Pink-1 (11). Therefore, we questioned whether a direct PS–PTEN–Pink-1 cascade could mechanistically account for PS-mediated modulation of Pink-1 or whether alternative pathways could be envisioned. As expected, PS1 overexpression enhances PTEN protein (Supplemental Figure S1A) and mRNA (Supplemental Figure S1C) expressions and transactivates its

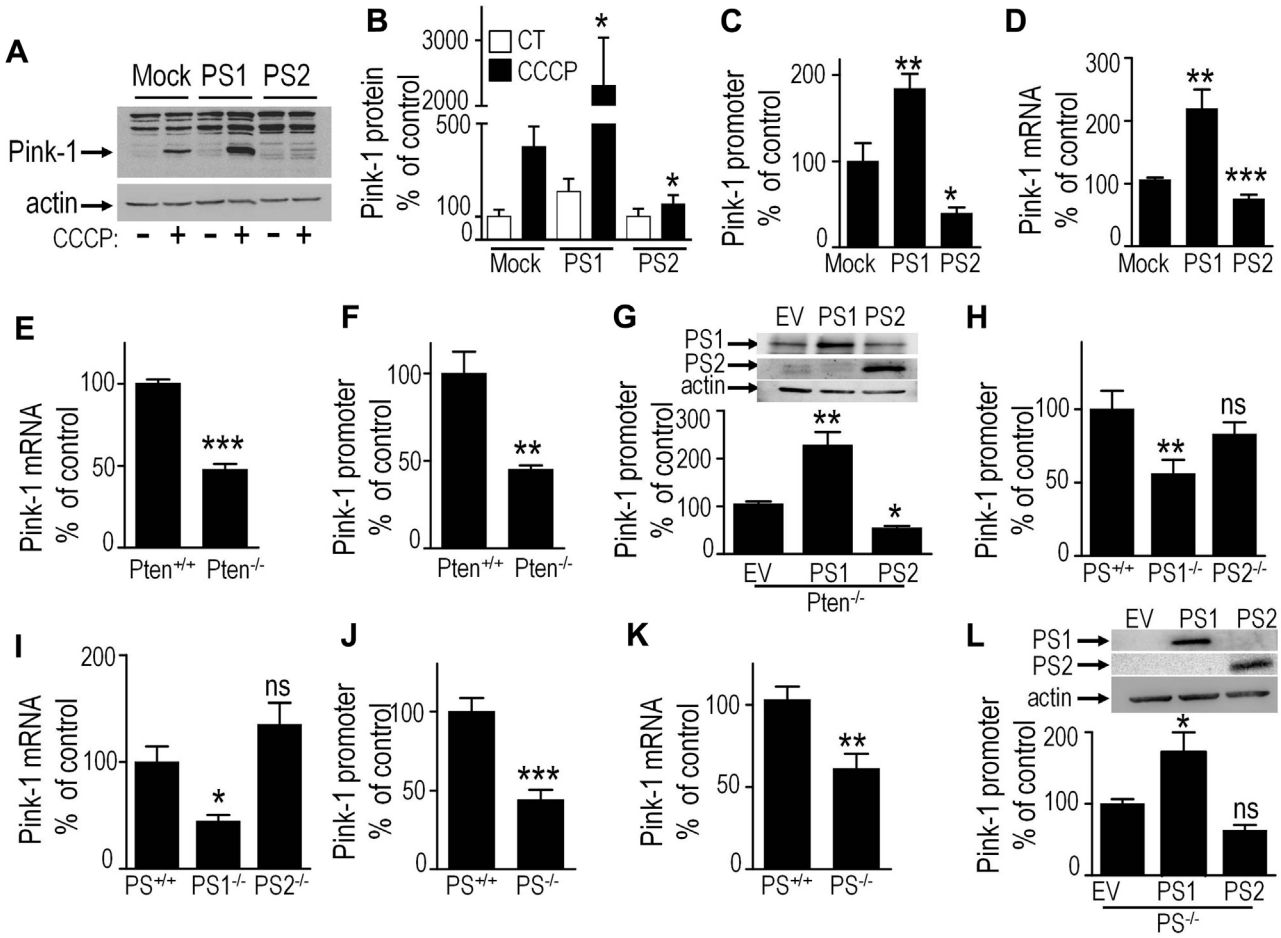

Figure 1. Phosphatase and tensin homolog (PTEN)-independent control of PTEN-induced kinase 1 (Pink-1) transcription by presenilin 1 (PS1). **(A, B)** Pink-1 and actin protein levels in human embryonic kidney 293 cells stably overexpressing an empty vector (EV) (Mock), PS1, and PS2 complementary DNA in basal (−, white bars) and carbonyl cyanide *m*-chlorophenyl hydrazone (CCCP)-treated (+, black bars) conditions. Representative gels **(A)** of pooled data (**B**, $n = 6$) are shown. **(C, D)** Pink-1 promoter activity (**C**, $n = 18$) and messenger RNA (mRNA) levels (**D**, $n = 9$) in the above-described cell models were measured as described in the experimental procedures. **(E–G)** Pink-1 mRNA levels (**E**, $n = 8$) and promoter activity (**F**, $n = 6$) in control ($PTEN^{+/+}$) or invalidated ($PTEN^{-/-}$) mouse embryonic fibroblast (MEF) cells. In **(G)**, Pink-1 promoter activity was measured in $PTEN^{-/-}$ cells after PS1 and PS2 overexpression ($n = 9$). Representative gels of PS1 and PS2 transfection efficiency and actin as gel charge control are provided in **(G)** (upper). **(H, I)** Pink-1 promoter activity (**H**, $n = 12$) and mRNA levels (**I**, $n = 6$) in control MEF cells ($PS^{+/+}$) or cells invalidated for either PS1 ($PS1^{-/-}$) or PS2 ($PS2^{-/-}$) were measured as described in the experimental procedures. **(J–L)** Pink-1 promoter activity (**J**, $n = 9$) and mRNA levels (**K**, $n = 12$) in control MEF cells ($PS^{+/+}$) or MEF cells devoid of both PS1 and PS2 ($PS^{-/-}$). In **(L)**, Pink-1 promoter activity was measured ($n = 7$) in $PS^{-/-}$ cells transiently transfected with either PS1 or PS2 complementary DNA as described in the experimental procedures. Representative gels of PS1 and PS2 transfection efficiency and actin as gel charge control are provided in **(L)** (upper panel). In all histograms, data are expressed as percentage of control (CT) taken as 100 and represent mean ± SEM (*$p < .05$; **$p < .01$; ***$p < .001$; ns, nonsignificant).

promoter (Supplemental Figure S1B), while depletion of endogenous PS1 triggers the opposite phenotype (Supplemental Figure S1D, E). It is noteworthy that PS2 expression lowers PTEN protein levels, promoter activity, and mRNA levels (Supplemental Figure S1A–C), a feature reminiscent of that observed for PS2-mediated control of Pink-1 (see Figure 1A–D). As expected, we also observed a drastic reduction of Pink-1 mRNA levels and promoter activation in PTEN-deficient fibroblasts (Figure 1E, F). Altogether, these data show that fibroblasts display canonical cellular responses linking PS and PTEN, on the one hand, and PTEN and Pink-1, on the other. However, we show that PS-mediated control of Pink-1 remained unaltered by PTEN gene invalidation (Figure 1G), indicating that PSs likely control Pink-1 transcription by alternative PTEN-independent pathways.

To rule out a possible artifactual influence of PS on Pink-1 due to the overexpression procedure, we examined the effect of endogenous PS on Pink-1 transactivation and mRNA levels. PS1 gene depletion lowers Pink-1 promoter transactivation (Figure 1H) and mRNA levels (Figure 1I), while PS2 gene ablation leads to barely detectable and not statistically significant effects (Figure 1H, I). The discrepancy between PS2 overexpression and depletion data could be explained by the previously described interplay between PS1 and PS2 (30). Thus, we showed that PS2 lowers PS1 expression. As such, PS2 overexpression via reduction of PS1 triggers Pink-1

diminution, while PS2 depletion remains biologically inert. This suggests a dominant role of PS1 over PS2 in the control of Pink-1. Indeed, invalidation of both PS1 and PS2 lowers both Pink-1 promoter activation (Figure 1J) and mRNA levels (Figure 1K), a phenotype similar to the one observed with PS1 depletion only (Figure 1H, I). In agreement, in a double PS1/2 knockout background, PS1 only rescues the Pink-1 activation of its promoter (Figure 1L). Overall, these data show that PS1 is involved in the transcriptional activation of Pink-1 by a PTEN-independent mechanism.

PS1-Mediated Control of Pink-1 Is Dependent on Its Catalytic Activity

PSs are pleiotropic proteins (31) but act as the catalytic core of γ-secretase, the enzymatic complex yielding Aβ (15). We examined, by pharmacological and mutational approaches, the consequences of the blockade of PS-mediated catalysis for Pink-1. Mutation on the aspartyl residue in position 257 of PS1 abolishes its activity (32) and reduces Pink-1 protein expression (Figure 2A), promoter activation (Figure 2B), and mRNA levels (Figure 2C). Furthermore, inhibition of γ-secretase by two distinct inhibitors [D6 (25) and DFK-167 (33)] led to similar reductions of Pink-1 protein expression (Figure 2D).

We examined whether pharmacological blockade of γ-secretase could also influence Pink-1 mRNA levels in vivo in triple transgenic mice model (3xTgAD harboring $PS1_{M146V}$, $βAPP_{swe}$, and TAU_{P301L} transgenes) of AD (26). Interestingly, 3xTgAD mice exhibit increased Pink-1 mRNA levels at 3 months of age [i.e., when C99 (the β-secretase–derived fragment of βAPP) accumulates in the absence of detectable Aβ (34)] and steadily until 12 months (Supplemental Figure S2A). Then, we examined the influence of pharmacological blockade of γ-secretase by D6 on Pink-1 mRNA levels. First, we confirmed that D6 treatment abolished γ-secretase activity as illustrated by complete inhibition of Aβ and AICD in vitro production (Supplemental Figure S3A), as previously described (34). As expected, D6 highly enhanced the expression of C-terminal fragment APP fragments C83 and C99 but also drastically reduced recovery of AICD in treated 3xTgAD brains (Supplemental Figure S3B). It is noteworthy that AICD expression was higher in 3xTgAD mice than in control wild-type mice (Supplemental Figure S3B). Of importance, D6 did not affect Pink-1 mRNA levels in control mice and restored Pink-1 mRNA expression to control mice levels in 3xTgAD mice (Figure 2E). It is noteworthy that PS-dependent control of PTEN (see above) was independent of its γ-secretase activity (18) and hence supports the dichotomy between γ-secretase-independent PS1-related effects on PTEN and γ-secretase-dependent effects on Pink-1. Overall, our data indicate that γ-secretase activity accounts for PS1-mediated control of Pink-1 both in vitro and in vivo.

PS-Mediated Control of Pink-1 Is Affected by βAPP Modulation

Besides βAPP, which originally allowed characterization of PS catalytic function (15), numerous proteins were delineated as additional γ-secretase substrates (17). Thus, we examined the contribution of βAPP to PS1-dependent control of Pink-1 in human cells. Wild-type βAPP overexpression augmented Pink-1 protein (Figure 3A) and mRNA (Figure 3C) expressions and led to enhanced Pink-1 promoter transactivation (Figure 3B). Interestingly, these augmentations were further enhanced in cells expressing the Swedish mutated βAPP (Supplemental Figure S4A–C). Conversely, mouse embryonic fibroblast cells that naturally lack endogenous βAPP family member APLP1 and that are genetically invalidated for both

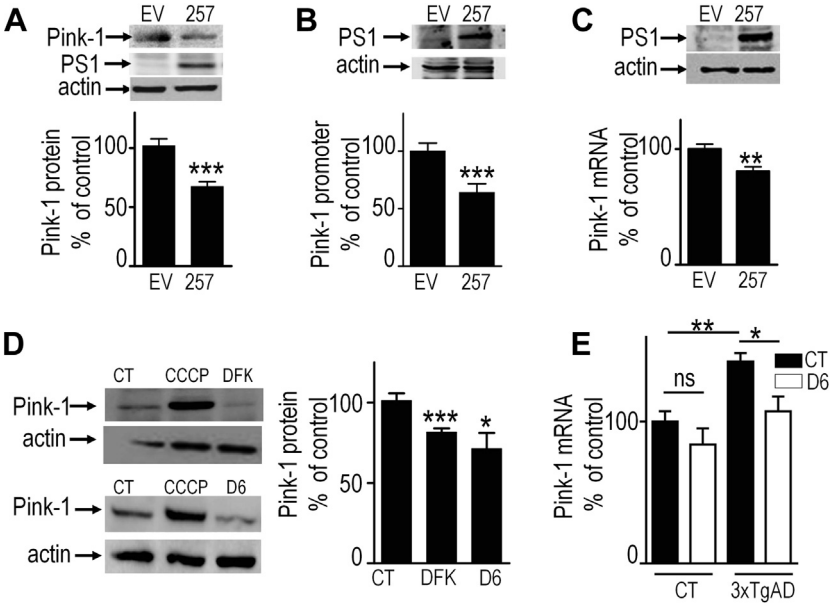

Figure 2. Phosphatase and tensin homolog–induced kinase 1 (Pink-1) control by presenilin 1 (PS1) is γ-secretase dependent. **(A–C)** Effect of the D257A PS1 mutation on Pink-1 protein (**A**, $n = 12$), promoter activity (**B**, $n = 9$), and messenger RNA (mRNA) levels (**C**, $n = 12$) after transient transfection of human embryonic kidney 293 cells with an empty vector (EV) or mutated complementary DNA (257). Representative gels of PS1 transfection efficiency and actin as gel charge control are provided in **(A)** to **(C)** (upper panels). **(D, E)** Modulation of Pink-1 expression by γ-secretase inhibitors ex vivo (**D**, $n = 12$) and in vivo (**E**, $n = 8–9$). In **(D)**, human embryonic kidney 293 cells were treated with DFK167 or DLN006 (D6) and then analyzed for Pink-1 expression by Western blot analysis as described in the experimental procedures. Representative gels of Pink-1 and actin of pooled data are provided in (**D**, left). In **(E)**, 4-month-old control (CT) and triple transgenic (3xTgAD) mice were daily treated for 10 days with a vehicle (CT, black bars) or with γ-secretase inhibitor (D6, white bars), and then Pink-1 mRNA levels ($n = 8–9$) were analyzed at 4 months of age as detailed in the experimental procedures. Data are expressed as percentage of CT taken as 100 and represent mean ± SEM (*$p < .05$; **$p < .01$; ***$p < .001$; ns, nonsignificant). CCCP, carbonyl cyanide *m*-chlorophenyl hydrazine.

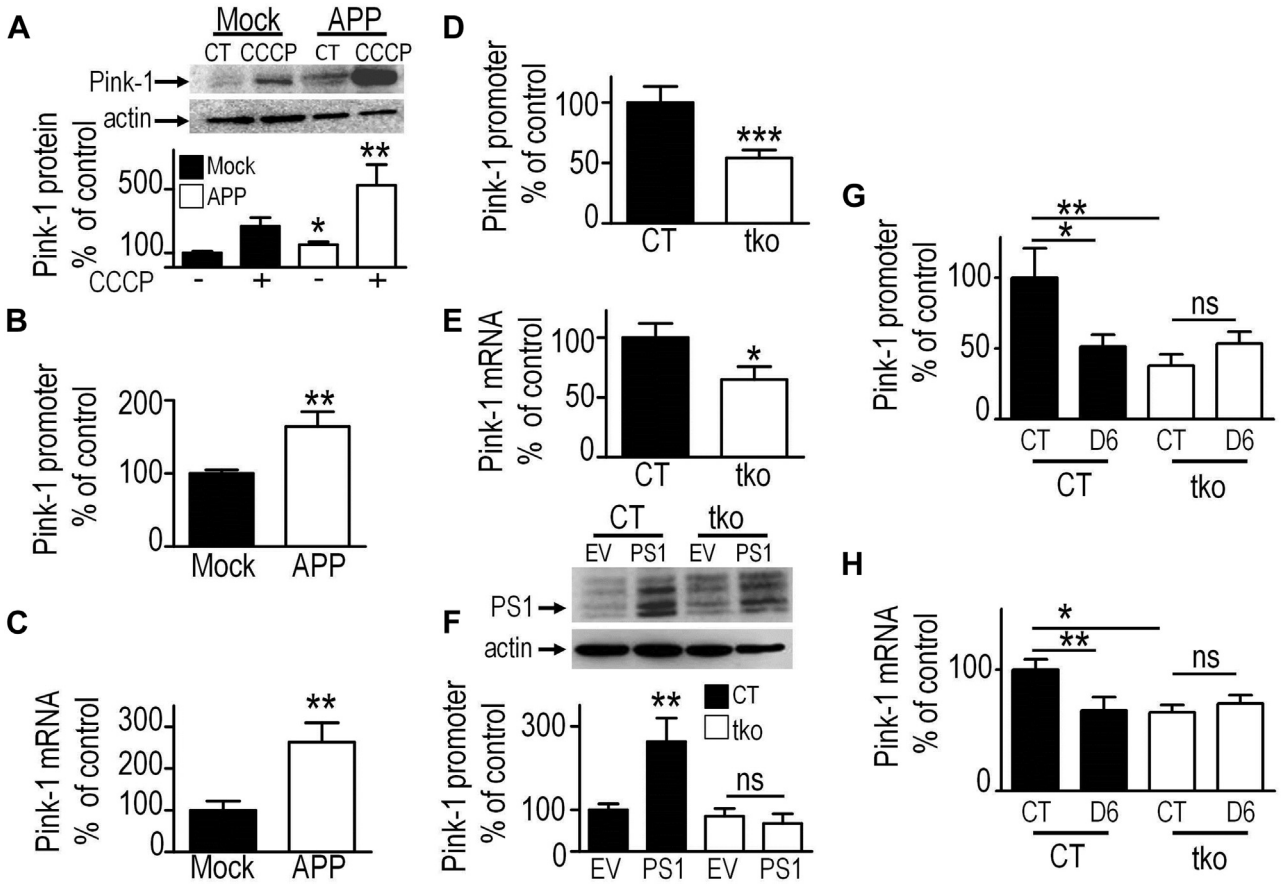

Figure 3. γ-Secretase-mediated control of phosphatase and tensin homolog–induced kinase 1 (Pink-1) is linked to β-amyloid precursor protein (βAPP) cleavage. **(A)** Pink-1 and actin protein levels in human embryonic kidney 293 cells stably overexpressing an empty vector (Mock, black bars) or wild-type βAPP (APP, white bars) in basal (−) and carbonyl cyanide *m*-chlorophenyl hydrazine (CCCP)-treated (+) conditions. Bars are means of $n = 12$. **(B, C)** Pink-1 promoter activity (**B**, $n = 12$) and messenger RNA (mRNA) levels (**C**, $n = 12$) in the above-described cell model were measured as indicated in the experimental procedures. **(D, E)** Pink-1 promoter activity (**D**, $n = 12$) and mRNA levels (**E**, $n = 9$) in control (CT, black bars) or triple knockout ($\beta APP^{-/-}$ and $APLP2^{-/-}$ and lacking endogenous APLP1 referred to as triple knockout (tko), white bars; see Results) mouse embryonic fibroblast cells were measured as indicated in the experimental procedures. **(F)** Pink-1 promoter activity was measured ($n = 6$) in either CT or tko mouse embryonic fibroblast cells transiently transfected with empty vector (EV) or presenilin 1 (PS1) complementary DNA. **(G, H)** Pink-1 promoter activity (**G**) and mRNA levels (**H**) in CT and tko mouse embryonic fibroblast cells were measured ($n = 6$) in the absence (CT) or presence of γ-secretase inhibitor (D6) as described in the experimental procedures. Data are expressed as percentage of CT taken as 100 and represent mean ± SEM (*$p < .05$; **$p < .01$; ***$p < .001$; ns, nonsignificant).

βAPP and its additional family member APLP2 (thus considered as triple knockout [tko] in Figure 3) show reduced Pink-1 promoter activity (Figure 3D) and mRNA levels (Figure 3E). Of importance, PS1 overexpression enhances Pink-1 promoter transactivation in wild-type (control) cells but not in tko cells (Figure 3F). Finally, D6 reduces Pink-1 promoter activation and mRNA levels in wild-type (control) fibroblasts but not in tko fibroblasts (Figure 3G, H). Altogether, the above data demonstrate that PS1-mediated and γ-secretase–linked control of Pink-1 occurs via the γ-secretase cleavage of endogenous βAPP.

AICD Controls Cellular Pink-1 Transcription in a FOXO3a-Dependent Manner

Both Aβ and AICD harbor transcription factor properties (35–37). However, several lines of reasoning and independent data led us to consider AICD as the main mediator of PS1-linked control of Pink-1. First, AICD is a transcription factor (17) that is mainly generated in the amyloidogenic pathway from its precursor C99 by γ-secretase (38–40). Second, expression of βAPP harboring the Swedish mutation thought to potentiate BACE1-mediated formation of C99 increases Pink-1 promoter transactivation and mRNA levels (Supplemental Figure S4A–C). Third, APPε, the APP fragment that undergoes β/γ-secretase cleavages, thereby leading Aβ (41), but that lacks AICD, did not modulate Pink-1 expression (Supplemental Figure S4D). Fourth, we previously designed 2xTgAD mice that were derived from intercrossing of the F1 progeny of 3xTgAD with wild-type mice (34). At late stages, 3xTgAD and 2xTgAD mice accumulate C99 and AICD to similar extents, while Aβ is present only at barely detectable levels in 2xTg mice (34) compared with 3xTgAD mice. Interestingly, 12-month-old 2xTgAD and

3xTgAD mice display similar increases of Pink-1 mRNA levels (Supplemental Figure S2B). Fifth, in vivo inhibitor-mediated full blockade of γ-secretase in 3xTgAD mouse brain (Supplemental Figure S3A) drastically reduces AICD expression (Supplemental Figure S3B) and concomitantly restores Pink-1 mRNA levels to control values (Figure 2E).

Based on these observations, therefore, we examined the putative influence of AICD on Pink-1. We used an AICD construct harboring a nuclear localization sequence (nls) aimed at potentiating its targeting to the nucleus. Figure 4 shows that AICD^{nls} (AICD) overexpression increases Pink-1 protein expression (Figure 4A), promoter transactivation (Figure 4B), and mRNA levels (Figure 4C). Figure 4D shows that AICD overexpression also increases Pink-1 promoter transactivation in tko fibroblasts.

We mapped the Pink-1 promoter region involved in its AICD-mediated transactivation. As expected, AICD increased transactivation of full-length Pink-1 promoter (cf. black and white full-length bars in Figure 4E). The 5′ deletions data indicated that deletion of the −2055- to −1354 Pink-1 promoter region fully abolished AICD-mediated increase in Pink-1 promoter activation (cf. full-length and 1.3 constructs in

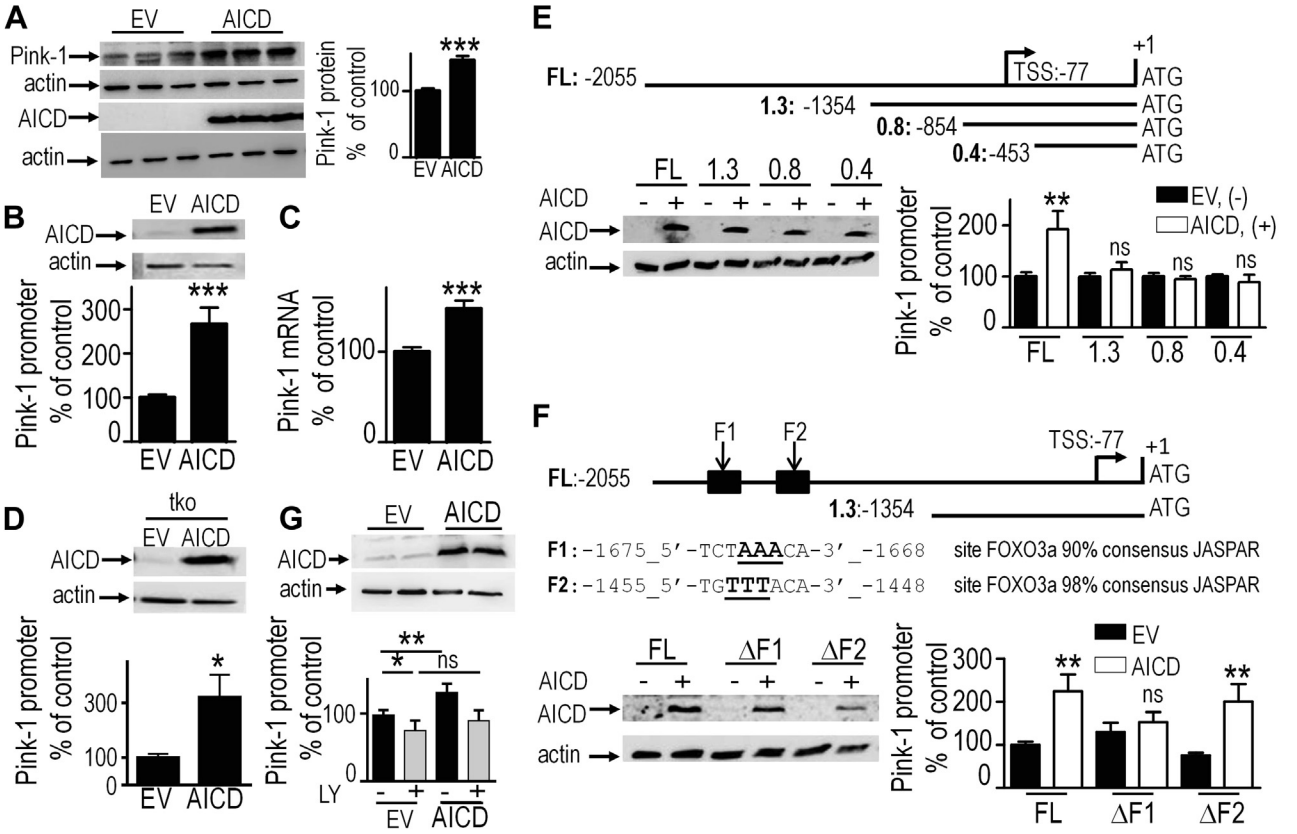

Figure 4. Amyloid precursor protein intracellular domain (AICD) controls phosphatase and tensin homolog–induced kinase 1 (Pink-1) transcription via Forkhead box O3a (FOXO3a). **(A–C)** Analysis of the effect of AICD^{nls} (referred to as AICD) on Pink-1 protein (**A,** n = 9), promoter activity (**B**, n = 15), and messenger RNA (mRNA) levels (**C,** n = 6) after transient transfection of human embryonic kidney 293 cells with empty vector (EV) or AICD^{nls} complementary DNA (cDNA). Representative gels of Pink-1, AICD^{nls}, and actin expressions are provided in (**A**, left). **(D)** Pink-1 promoter activity was measured (n = 10) in triple knockout mouse embryonic fibroblast cells on EV or AICD^{nls} cDNA transient transfection. Representative gels of AICD cDNA transfection efficiency and actin as gel charge control are provided in the left panel. **(E)** Mapping of the functional interaction domain of AICD and Pink-1 promoter. The upper panel represents the 5′ end deletion constructs of the full-length (FL) mouse Pink-1 promoter region. Pink-1 promoter constructs were cotransfected with the β-galactosidase reporter gene and either empty cDNA (EV, black bars, −) or AICD (white bars, +) cDNA, and then luciferase activity was measured (lower right, n = 9) as described in the experimental procedures. The lower left panel shows representative gels of AICD cDNA transfection efficiency and actin as gel charge control. **(F)** AICD controls Pink-1 transcription via FOXO3a. The upper panel describes the two putative FOXO3a binding consensus motifs identified, by the in silico approach, in the -2055- to -1353 region of the FL Pink-1 mouse promoter (referred to as F1 and F2). The effect of empty vector (EV, black bars, −) or AICD^{nls} (white bars, +) on FL or deleted F1 (ΔF1) or F2 (ΔF2) Pink-1 promoters was analyzed as above in **(F)** (lower right panel, n = 18). The lower left panel shows representative gels of AICD transfection efficiency and actin as gel charge control. **(G)** Effect of LY294002 (LY) on AICD-induced modulation of Pink-1 promoter activity. Pink-1 promoter constructs were cotransfected with the β-galactosidase reporter gene and either empty complementary DNA (EV) or AICD^{nls} (AICD) complementary DNA. One full day (24 hours) after transfection, cells were treated for 15 hours with either vehicle (−, black bars) or 10 μM LY294002 (LY, +, gray bars), and then luciferase activity (n = 12) was measured as described in Methods and Materials. The upper panel of **(G)** shows representative gels of AICD transfection efficiency and actin as gel charge control. Data are expressed as percentage of controls (EV, EV (−) or FL condition) taken as 100 and represent mean ± SEM (*$p < .05$; **$p < .01$; ***$p < .001$; ns, nonsignificant). ATG, methionine starting codon; nls, nuclear localization sequence; TSS, transcription start site.

Figure 4E). The close examination of this region allowed us to identify two FOXO3a responsive elements (F1 and F2) located within this functionally relevant 5′ region of Pink-1 promoter (Figure 4F, upper scheme). Our interest for FOXO3a was motivated by two independent observations. First, FOXO3a activation was previously shown to upregulate Pink-1 transcription in both mouse and human cells (42). Second, Wang *et al.* recently demonstrated a physical and functional interaction between FOXO3a and AICD (43). In this context, we postulated that FOXO3a and AICD could functionally interact to control Pink-1 transcription. Thus, we examined the influence of the mutation of these FOXO3a responsive elements on the AICD-mediated control of Pink-1. Our data indicate that between the two sites, only the F1 responsive element fully abolishes AICD-mediated transactivation of Pink-1 promoter (Figure 4F, lower right panel). These data were corroborated by experiments aimed at pharmacologically blocking FOXO3a with LY294002 (cf. gray bars in Figure 4G), showing that this inhibitor fully prevents AICD-induced increase in Pink-1 promoter activity. Overall, our data unravel a linear molecular cascade linking PS1, βAPP/AICD, FOXO3a, and Pink-1.

PK Controls Pink-1 Transcription in a PS-Dependent and PTEN-Independent Pathway

We previously demonstrated that besides its well-characterized ubiquitin-ligase activity (44), PK also behaved as a transcription factor (45). We showed that, among its various targets, PK directly upregulated PS1 and downregulated PS2 promoter transactivations and protein expressions (22). These opposite effects of PK on PS, which were strikingly similar to the opposite effects of PS1 and PS2 on Pink-1 transactivation (see Figure 1), led us to question whether PK could modulate Pink-1 transcription via PS1. Five lines of direct and indirect evidence support this hypothesis. First, PK overexpression increases Pink-1 promoter transactivation and mRNA levels (Figure 5A, B). Second, deletion of endogenous PK reduces Pink-1 transcription and mRNA expression ex vivo (Figure 5C, D). Third, Pink-1 protein and mRNA expression were lowered in the brain of PK null mice (Figure 5E, F). Fourth, PK-induced increment in Pink-1 promoter activation was fully abolished by *PS1* and *PS2* ($PS^{-/-}$) gene invalidation (Figure 5G). Fifth, PK ability to upregulate Pink-1 promoter transactivation remains unaffected by PTEN depletion (Figure 5H). While the control of PK by Pink-1 has been consistently documented (46,47), our data demonstrate, for the first time, a reciprocal pathway where PK acts upstream of a PS1/AICD-dependent cellular cascade linking PK to Pink-1.

AICD Modulates Mitochondrial Physiology in a Pink-1-Dependent Manner

If the above cascade is true, one anticipates an AICD-associated modulation of Pink-1–mediated functions. Pink-1 has been consistently involved in the control of mitophagy and mitochondrial dynamics (9).

Mitochondrial membrane potential directly reflects mitochondrial health and can be classically measured to follow mitophagy. First, we used tetramethyl-rhodamine methyl ester as an indicator of mitochondrial membrane potential alterations to analyze the impact of endogenous Pink-1 reduction on mitochondrial function. As expected (48), both confocal

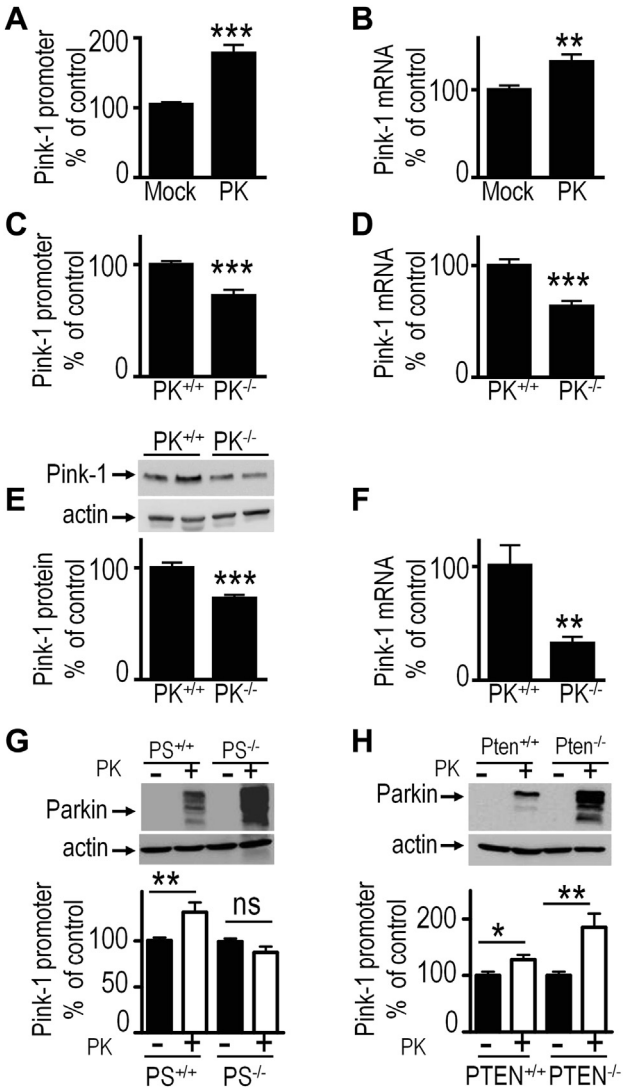

Figure 5. Parkin (PK) controls phosphatase and tensin homolog (PTEN)-induced kinase 1 (Pink-1) transcription via presenilin 1 in a PTEN-independent manner. **(A, B)** Pink-1 promoter activity (**A**, $n = 9$) and messenger RNA (mRNA) levels (**B**, $n = 12$) measurements in human embryonic kidney 293 cells stably overexpressing either a control vector (Mock) or wild-type PK. **(C, D)** Pink-1 promoter activity (**C**, $n = 12$) and mRNA levels (**D**, $n = 17$) analyses in control ($PK^{+/+}$) or parkin gene knockout ($PK^{-/-}$) mouse embryonic fibroblast cells. **(E, F)** Pink-1 protein (**E**, $n = 6$) and mRNA levels (**F**, $n = 6$) analyses in $PK^{+/+}$ or $PK^{-/-}$ mouse brain. **(G, H)** Pink-1 promoter activity analyses in presenilin $(PS)^{+/+}$ and $PS^{-/-}$ (**G**, $n = 18$) or $PTEN^{+/+}$ and $PTEN^{-/-}$ (**H**, $n = 6$) mouse embryonic fibroblast cells transiently overexpressing either an empty vector (−, black bars) or wild-type PK (+, white bars). Data are expressed as percentage of controls taken as 100 and represent mean ± SEM (*$p < .05$; **$p < .01$; ***$p < .001$; ns, nonsignificant).

(Figure 6A, B) and fluorescence-activated cell sorting (Figure 6C) analyses indicate that short hairpin RNA–induced Pink-1 knockdown in SH-SY5Y cells ($Pink\text{-}1^{KD}$) or full genetic depletion ($Pink\text{-}1^{-/-}$) in fibroblasts (Supplemental Figure S5) significantly reduced mitochondrial membrane potential (cf. black and white control bars in Figure 6B, C and

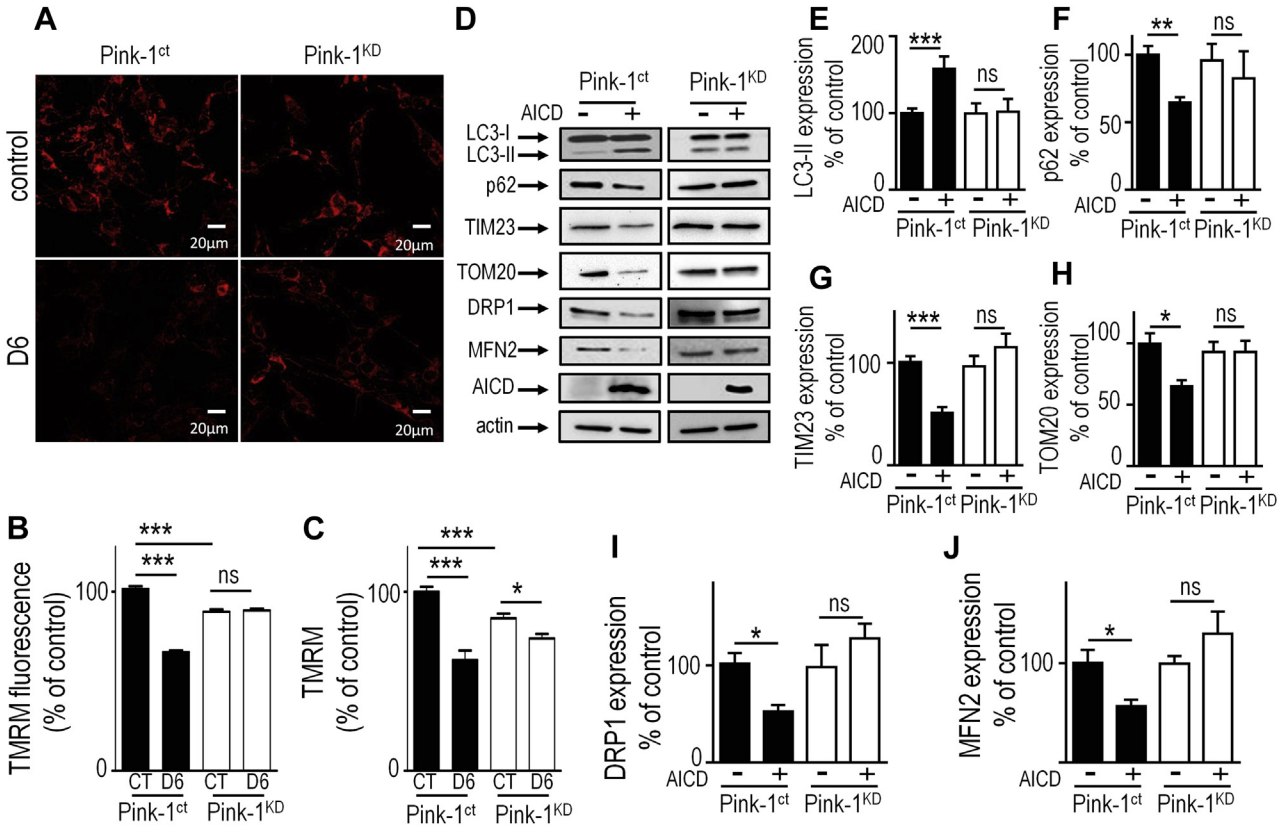

Figure 6. Amyloid precursor protein intracellular domain (AICD) controls mitochondrial homeostasis via phosphatase and tensin homolog–induced kinase 1 (Pink-1). **(A–C)** Control (Pink-1^{ct}, black bars) or short hairpin RNA-depleted Pink-1 (Pink-1^{KD}, white bars) SH-SY5Y cells were treated with the γ-secretase inhibitor ELND006 (D6), and its effect on mitochondrial potential was measured by cell imaging (**A**, **B**, $n = 150$ cells per experiment) and flow cytometry (**C**, $n = 12$) as detailed in the experimental procedures. **(D–J)** Impact of control (empty vector) or AICD^{nls} overexpression on autophagy LC3-II (**E**, $n = 9$) and p62 (**F**, $n = 9$), mitochondrial mass TIM23 (**G**, $n = 9$) and TOM20 (**H**, $n = 9$), and mitochondrial dynamics-related proteins dynamin-like protein 1 (DRP1) (**I**, $n = 9$) and mitofusin 2 (MFN2) (**J**, $n = 9$) markers was analyzed in Pink-1^{ct} (black bars) or Pink-1 knockdown (Pink-1^{KD}, white bars) SH-SY5Y cells as described in the experimental procedures. Representative gels of markers, AICD transfection efficiency, and actin (as gel charge control) are provided in indicated cells **(D)**. Data in histograms are expressed as percentage of controls taken as 100 and represent mean ± SEM (*$p < .05$; **$p < .01$; ***$p < .001$; ns, nonsignificant). CT, control; nls, nuclear localization sequence; TMRM, tetramethyl-rhodamine methyl ester.

Supplemental Figure S5B). It is noteworthy that the D6 reduced tetramethyl-rhodamine methyl ester fluorescence in wild-type cells, a phenotype abolished by endogenous Pink-1 depletion in both Pink-1^{KD} and Pink-1$^{-/-}$ cells (Figure 6B, C and Supplemental Figure S5, respectively). This effect was confirmed by use of another γ-secretase inhibitor, DFK167, in Pink-1$^{-/-}$ fibroblasts (Supplemental Figure S5). This set of data clearly indicates that Pink-1-mediated control of mitophagy/autophagy is modulated by γ-secretase–linked events in these cells. To directly link this function to AICD, we examined the influence of AICD^{nls} on LC3II and p62, two classical markers of autophagosome formation and autophagic degradation, respectively. First, we confirmed that reduction of Pink-1 in Pink-1^{KD} cells (Supplemental Figure S6A–C) modulated p62 and LC3II expressions in an opposite manner in stress conditions (CCCP in Supplemental Figure S6D–F), suggesting a decreased autophagic process as previously described (49,50). Interestingly, AICD^{nls} overexpression increased LC3II (cf. black bars in Figure 6D, E) and reduced p62 (cf. black bars in Figure 6D, F) levels in wild-type SH-SY5Y cells but not in Pink-1^{KD} cells (cf. white bars in Figure 6D–F), indicating that AICD^{nls} promotes a pro-autophagic phenotype that is fully dependent on endogenous Pink-1. It is noteworthy that FOXO3a controls autophagy via its transcription factor properties (51,52). Thus, it is not excluded that AICD/FOXO3a interaction may alter expressions of additional genes involved in nonselective autophagy. To foster the implication of AICD in mitophagy control, we have analyzed its impact on the levels of TIM23 and TOM20, two reliable markers of mitochondrial mass used to follow the mitophagy process (53,54). First, we confirmed that Pink-1 depletion triggers accumulation of TIM23 (Supplemental Figure S6D, G) and TOM20 (cf. white bars in Supplemental Figure S6D, H) levels in CCCP conditions. Interestingly, AICD^{nls} overexpression decreased TIM23 (cf. black bars in Figure 6D, G) and TOM20 (cf. black bars in Figure 6D, H) levels in wild-type SH-SY5Y cells but not in Pink-1^{KD} cells (Figure 6D and cf. white bars in Figure 6G, H).

Finally, mitochondrial dynamics are mainly supported by fusion/fission processes that can be followed by canonical markers such as mitofusin 2 and dynamin-like protein 1. (1). We confirmed that Pink-1 knockdown leads to accumulation of

mitofusin 2 and dynamin-like protein 1 levels (Supplemental Figure S6I–K), probably due to the decrease of Pink-1–mediated PK recruitment and E3-ligase activity (55,56). Again, conversely, AICD^{nls} expression reduces dynamin-like protein 1 and mitofusin 2 expressions in Pink-1 control cells (Figure 6D, I, J), a phenotype fully prevented by Pink-1 knockdown (Figure 6D, I, J). The above data indicate that both γ-secretase inhibition and AICD^{nls} expression modulate mitophagy and mitochondrial dynamics in a Pink-1-dependent manner, thereby confirming AICD as a potent modulator of Pink-1-mediated phenotypes.

AICD Modulates Pink-1 Transcription In Vivo

To reinforce our cell biology approaches, we examined whether AICD could modulate Pink-1 protein and mRNA levels in vivo in mouse brain. First, we used an adenoviral approach to express AICD^{nls} in neonatal mouse brain. As illustrated in Figure 7A, AICD^{nls} is expressed in hippocampal regions (1 month old) and appears to be clearly associated with 4′,6-diamidino-2-phenylindole nuclear labeling (Figure 7A, lower panels), indicating its efficient nuclear translocation in vivo. AICD^{nls} increased expressions of Pink-1 protein (Figure 7B) and mRNA levels of Pink-1 and neprilysin, a canonical AICD transcriptional target (20) (Figure 7C). Second, we analyzed the impact of AICD in a transgenic mice model stably overexpressing AICD (57,58). As previously described (59), AICD-Tg mice display enhanced neprilysin mRNA levels (Figure 7E) and increased Pink-1 protein expression and mRNA levels (Figure 7D, E). Altogether, these two independent mice models of AICD expression concur to conclude that AICD acts as a genuine modulator of Pink-1 promoter transactivation in cells and in vivo.

DISCUSSION

Specific histological lesions serve as anatomical signatures to characterize subsets of neurodegenerative diseases. However,

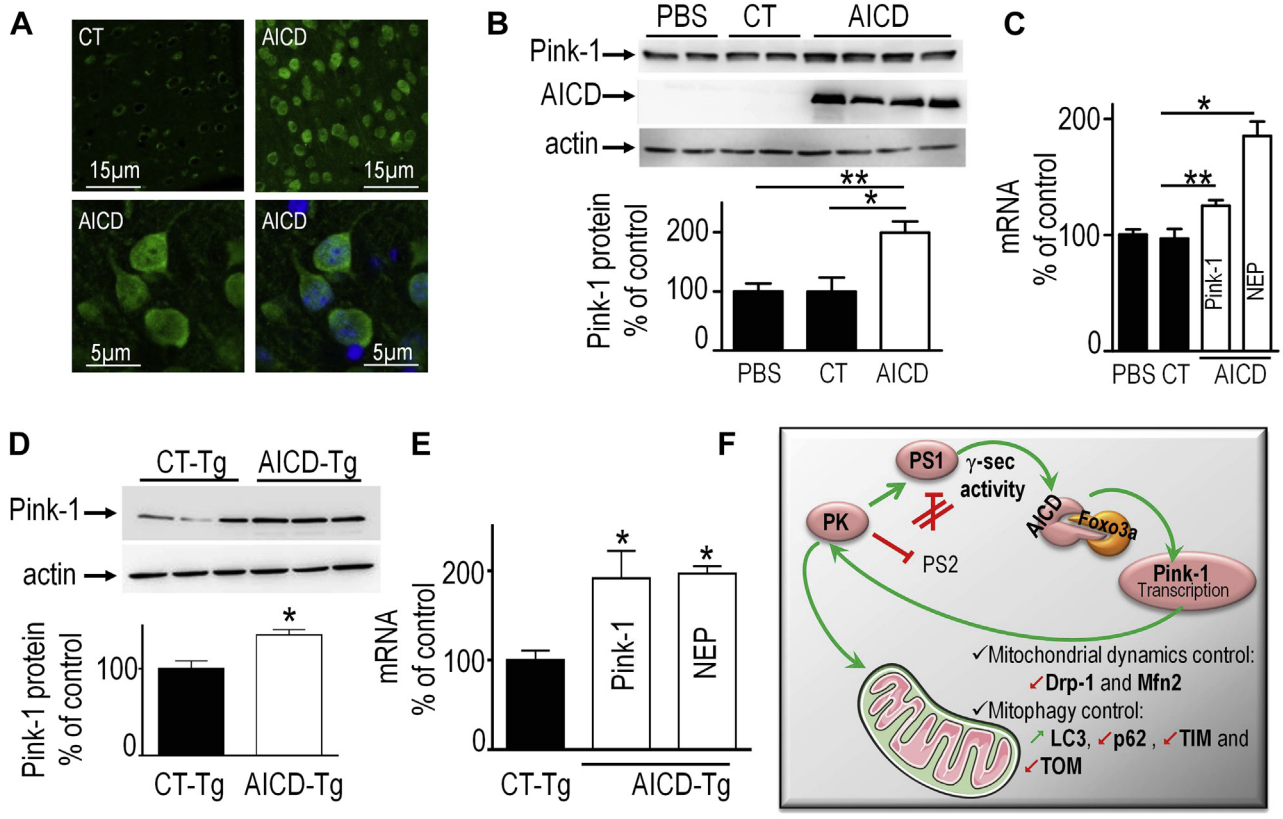

Figure 7. Amyloid precursor protein intracellular domain (AICD) controls phosphatase and tensin homolog–induced kinase 1 (Pink-1) transcription in vivo. **(A)** Low (upper panel) and high (lower panel) magnification of immunohistochemical analyses of adeno-associated virus-AICD^{nls} intranuclear localization in the subiculum of 1-month-old C57BL/6 mice injected at postnatal day 1 as described in the experimental procedures. Green and blue fluorescences correspond to AICD and 4′,6-diamidino-2-phenylindole nuclear labeling, respectively. **(B, C)** Analysis (at 4 months of age) of the effect of AICD^{nls} overexpression after neonatal adeno-associated virus-mediated delivery on Pink-1 protein (**B**, n = 4–9) and Pink-1 and neprilysin (NEP) messenger RNA (mRNA) (**C**, n = 8–17, white bars) levels compared with age-matched administration of control virus (CT) or virus vehicle (PBS). Data in histograms are expressed as percentage of controls taken as 100 and represent mean ± SEM (*$p < .05$; **$p < .01$). **(D, E)** Pink-1 protein (**D**, n = 3) and Pink-1 and NEP mRNA levels (**E**, n = 3) in age-matched (13 months) control (CT-Tg) and AICD-Tg mouse brain. Data in histograms are expressed as percentage of controls taken as 100 and represent mean ± SEM (*$p < .05$). **(F)** Model of the molecular interplay linking parkin (PK) and Pink-1. PK upregulates presenilin 1 (PS1)/γ-secretase activity, thereby promoting Forkhead box O3a (FOXO3a)-dependent AICD-mediated control of Pink-1 transcriptional regulation. Because Pink-1 recruits PK to modulate mitochondrial dynamics and mitophagy, the functional interplay between PK and Pink-1 supports their cellular homeostasis and thereby controls mitochondria physiology and governs their responsiveness and adaptation to pathological conditions. Drp-1, dynamin-like protein 1; Mfn2, mitofusin 2; PS2, presenilin 2.

additional dysfunctions such as protein aggregation (60,61), misfolding and more recently spreading (62), proteasome dysfunction (63), endoplasmic reticulum stress and unfolded protein response activation (64), as well as other vital cellular processes, are also seen as common denominators of brain diseases. It has also been suggested that mitochondrial dysfunctions could well underlie at least part of neurodegenerative processes. Thus, disruption of mitochondrial dynamics reflected by altered balance between fission and fusion processes or inefficient mitochondria quality control by mitophagy has been consistently reported (1,2). Such defects have been described in AD (65), but the molecular mechanisms underlying these observations remained poorly understood.

Pink-1 is a kinase that harbors a dual mitochondrial and cytosolic localization. Among Pink-1–related functions, its involvement in the control of mitochondria morphology was first documented (66), and then Pink-1 was shown to control the mitophagy process (49). Interestingly, Pink-1-like immunoreactivity colocalized with senile plaques in AD-affected brains (67). These data led us to examine the mechanisms by which Pink-1 could account for the mitochondrial dynamics and mitophagy alterations taking place in AD.

We delineated a molecular cascade linking PS1 and Pink-1. Thus, overexpression/depletion of PS1 increases/lowers Pink-1 promoter transactivations and mRNA and protein expressions. Cellular biology and pharmacological approaches, as well as in vivo models, indicate that PS1-mediated control of Pink-1 involved γ-secretase cleavage of βAPP. Furthermore, we identified AICD as the cellular mediator able to modulate Pink-1 transactivation in cells, as well as in vivo, in two distinct models of AICD-expressing mice. It is noteworthy that AICD modulates Pink-1-associated changes in mitochondrial membrane potential and autophagy/mitophagy players' expression. Importantly, we established that PS1-mediated control of Pink-1 was independent of PTEN. These data agree well with a prior study showing that, conversely to PS1-mediated control of Pink-1, PS1 modulation of PTEN was independent of γ-secretase (18). Thus, PS1-dependent modulation of Pink-1 and PTEN appear to be either linked to or independent of its catalytic function.

AICD is a transcription factor able to modulate transcription of a number of genes (17,21,68). Such function is often supported by AICD ability to interact with cofactors/nuclear modulators (17,68). Here, we demonstrated that AICD-associated control of Pink-1 involved FOXO3a given that deletion of FOXO3a responsive elements on Pink-1 promoter fully abolished AICD-induced modulation of its transcription. These data agree well with a previous study showing that AICD and FOXO3a interacted physically and translocated in the nucleus to ultimately control cell death (43). Furthermore, FOXO3a regulated Pink-1 transcription in human cells (42). This adds to the growing evidence that epigenetic factors could well contribute to aging and dementia (69,70).

It is interesting to note that two previous studies indirectly suggested a putative functional link between AICD and Pink-1 in the control of mitochondrial function. Thus, the mRNA levels of PGC-1α, a mitochondrial coactivator driving the expression of various mitochondrial proteins, were lowered by PS1 pathogenic mutations and upregulated by AICD (71), while Pink-1 also increased PGC-1α-linked regulation of mitochondrial oxidation (72).

Recent evidence indicates that Pink-1 controls mitochondrial fragmentation in hippocampal neurons (9) and recruits PK to damaged mitochondria to trigger mitophagy (10). In both cases, Pink-1 has been considered as an effector acting upstream of PK. Our study demonstrates that PK could also occur upstream of Pink-1 to regulate its function. Initially, this hypothesis was based on our previous study showing that PK could behave as a direct transactivator that up- or downregulated PS1 and PS2 promoter transactivation, respectively (22). This opposite effect of PK on PS1 and PS2 was strikingly reminiscent of the PS1/PS2-mediated effect on Pink-1 (see Figure 1). Interestingly, we were able to show, first, that PK overexpression or deletion increased or lowered Pink-1 promoter transactivation and mRNA levels, respectively, and, second, that PK-mediated control of Pink-1 was fully abolished by PS depletion and remains independent of PTEN. Thus, we have evidenced a functional interplay between PK and Pink-1 and unraveled a key role of PS1/γ-secretase–derived AICD fragment in such regulation (see Figure 7F).

The above-described cascade and feedback loop could ensure protein homeostasis in physiological conditions and adjust cellular responses to control mitochondrial physiology in case of cellular stresses or challenges. This interplay could be of importance in neurodegenerative diseases. Thus, we showed that several PK mutations responsible for familial Parkinson's disease abolish its transcriptional function (45). In these cases, lowering PS1 could ultimately drive reduction of Pink-1 and thereby compromise the adaptive response to mitochondrial dysfunction. On the other hand, in both sporadic and most familial cases of AD, AICD expression is likely increased due to either a lower degradation rate linked to reduced expression of its insulin-degrading enzyme (73) or increased production triggered by APP or PS1 mutations (74). This could explain the macroscopic observation of an increased expression of Pink-1 in senile plaques and reflect a cellular adaptation response to circumscribe the neurodegenerative process. Overall, our study enlightens a novel cellular cascade and delineates potential targets for therapeutic intervention.

ACKNOWLEDGMENTS AND DISCLOSURES

This work was supported by the Conseil départemental des Alpes Maritimes and the Foundation Claude Pompidou. This work was developed and supported through the LABEX (Laboratory of Excellence, Investments for the Future) DISTALZ (Development of Innovative Strategies for a Transdisciplinary Approach to Alzheimer's Disease) and the Hospital University Federation OncoAge. TG is funded by the Ligue Contre le Cancer.

We sincerely thank A.Y. Abramov, O. Corti, T. Dawson, B. de Strooper, F. LaFerla, and U. Muller for providing valuable cellular and animal models, and we thank G. Thinakaran and Elan Pharmaceuticals for providing the anti-PS antibody and γ-secretase inhibitor D6, respectively.

The authors report no biomedical financial interests or potential conflicts of interest.

ARTICLE INFORMATION

From the Institut de Pharmacologie Moléculaire et Cellulaire (TG, ED, MC, AB, WEM, LR, JD, IL, RP-P, FC, CAdC), Université Côte d'Azur, Centre

National de la Recherche Scientifique (CNRS), Institut National de la Santé et de la Recherche Médicale (INSERM), Valbonne; Center of Research on Myology (M-GB, MB), Pierre and Marie Curie University, CNRS, INSERM, Paris; and Alzheimer & Taopathies (NS, MC), Jean-Pierre Aubert Research Centre, Faculté de Médecine, L'Institut de Médecine Prédictive et de Recherche Thérapeutique, INSERM, Lille, France; State Key Laboratory of Cellular Stress Biology (HY), Innovation Center for Cell Signaling Network, School of Life Sciences, Xiamen University, Xiamen, Fujian, China; Princess Margaret Center (VS), University Health Network and Department of Medical Biophysics, University of Toronto, Toronto, Ontario, Canada; Department of Neurosciences (SWP), Lerner Research Institute, Cleveland Clinic, Cleveland, Ohio; and Instituto de Medicina Molecular (VAM), Faculdade de Medicina, Universidade de Lisboa, Lisbon, Portugal.

FC and CAdC contributed equally to this work.

Address correspondence to Cristine Alves da Costa, Ph.D., UMR 7275, 660 Route des Lucioles, Valbonne 06560, France; E-mail: acosta@ipmc.cnrs.fr.

Received Aug 26, 2016; revised Apr 10, 2017; accepted Apr 22, 2017.

Supplementary material cited in this article is available online at http://dx.doi.org/10.1016/j.biopsych.2017.04.011.

REFERENCES

1. Chen H, Chan DC (2009): Mitochondrial dynamics—fusion, fission, movement, and mitophagy—in neurodegenerative diseases. Hum Mol Genet 18:R169–R176.
2. Son JH, Shim JH, Kim KH, Ha JY, Han JY (2012): Neuronal autophagy and neurodegenerative diseases. Exp Mol Med 44:89–98.
3. Swerdlow RH, Burns JM, Khan SM (2014): The Alzheimer's disease mitochondrial cascade hypothesis: Progress and perspectives. Biochim Biophys Acta 1842:1219–1231.
4. Gibson GE, Starkov A, Blass JP, Ratan RR, Beal MF (2010): Cause and consequence: Mitochondrial dysfunction initiates and propagates neuronal dysfunction, neuronal death, and behavioral abnormalities in age-associated neurodegenerative diseases. Biochim Biophys Acta 1802:122–134.
5. Baloyannis SJ (2006): Mitochondrial alterations in Alzheimer's disease. J Alzheimers Dis 9:119–126.
6. Trushina E, Nemutlu E, Zhang S, Christensen T, Camp J, Mesa J, *et al.* (2012): Defects in mitochondrial dynamics and metabolomic signatures of evolving energetic stress in mouse models of familial Alzheimer's disease. PLoS One 7:e32737.
7. Calkins MJ, Manczak M, Mao P, Shirendeb U, Reddy PH (2011): Impaired mitochondrial biogenesis, defective axonal transport of mitochondria, abnormal mitochondrial dynamics and synaptic degeneration in a mouse model of Alzheimer's disease. Hum Mol Genet 20:4515–4529.
8. Boland B, Kumar A, Lee S, Platt FM, Wegiel J, Yu WH, *et al.* (2008): Autophagy induction and autophagosome clearance in neurons: Relationship to autophagic pathology in Alzheimer's disease. J Neurosci 28:6926–6937.
9. Yu W, Sun Y, Guo S, Lu B (2011): The PINK1/Parkin pathway regulates mitochondrial dynamics and function in mammalian hippocampal and dopaminergic neurons. Hum Mol Genet 20:3227–3240.
10. Matsuda N, Sato S, Shiba K, Okatsu K, Saisho K, Gautier CA, *et al.* (2010): PINK1 stabilized by mitochondrial depolarization recruits parkin to damaged mitochondria and activates latent parkin for mitophagy. J Cell Biol 189:211–221.
11. Unoki M, Nakamura Y (2001): Growth-suppressive effects of BPOZ and EGR2, two genes involved in the PTEN signaling pathway. Oncogene 20:4457–4465.
12. Sonoda Y, Mukai H, Matsuo K, Takahashi M, Ono Y, Maeda K, *et al.* (2010): Accumulation of tumor-suppressor PTEN in Alzheimer neurofibrillary tangles. Neurosci Lett 471:20–24.
13. Knafo S, Sanchez-Puelles C, Palomer E, Delgado I, Draffin JE, Mingo J, *et al.* (2016): PTEN recruitment controls synaptic and cognitive function in Alzheimer's models. Nat Neurosci 19:443–453.
14. Wilhelmus MM, van der Pol SM, Jansen Q, Witte ME, van der Valk P, Rozemuller AJ, *et al.* (2011): Association of Parkinson disease-related protein PINK1 with Alzheimer disease and multiple sclerosis brain lesions. Free Radic Biol Med 50:469–476.
15. De Strooper B, Saftig P, Craessaerts K, Vanderstichele H, Guhde G, Annaert W, *et al.* (1998): Deficiency of presenilin-1 inhibits the normal cleavage of amyloid precursor protein. Nature 391:387–390.
16. Wolfe MS, Haass C (2001): The role of presenilins in γ-secretase activity. J Biol Chem 276:5413–5416.
17. Pardossi-Piquard R, Checler F (2012): The physiology of the beta-amyloid precursor protein intracellular domain AICD. J Neurochem 120(suppl 1):109–124.
18. Zhang H, Liu R, Wang R, Hong S, Xu H, Zhang YW (2008): Presenilins regulate the cellular level of the tumor suppressor PTEN. Neurobiol Aging 29:653–660.
19. Gao Y, Pimplikar SW (2001): The γ-secretase-cleaved C-terminal fragment of amyloid precursor protein mediates signaling to the nucleus. Proc Natl Acad Sci U S A 98:14979–14984.
20. Pardossi-Piquard R, Petit A, Kawarai T, Sunyach C, Alves da Costa C, Vincent B, *et al.* (2005): Presenilin-dependent transcriptional control of the Abeta-degrading enzyme neprilysin by intracellular domains of betaAPP and APLP. Neuron 46:541–554.
21. Konietzko U (2012): AICD nuclear signaling and its possible contribution to Alzheimer's disease. Curr Alzheimer Res 9:200–216.
22. Duplan E, Sevalle J, Viotti J, Goiran T, Bauer C, Renbaum P, *et al.* (2013): Parkin differently regulates presenilin-1 and presenilin-2 functions by direct control of their promoter transcription. J Mol Cell Biol 5:132–142.
23. Zhang X, Tang N, Hadden TJ, Rishi AK (2011): Akt, FoxO and regulation of apoptosis. Biochim Biophys Acta 1813:1978–1986.
24. Giaime E, Sunyach C, Druon C, Scarzello S, Robert G, Grosso S, *et al.* (2010): Loss of function of DJ-1 triggered by Parkinson's disease-associated mutation is due to proteolytic resistance to caspase-6. Cell Death Differ 17:158–169.
25. Probst G, Aubele DL, Bowers S, Dressen D, Garofalo AW, Hom RK, *et al.* (2013): Discovery of (*R*)-4-cyclopropyl-7,8-difluoro-5-(4-(trifluoromethyl)phenylsulfonyl)-4,5-dihydro-1*H*-pyrazolo[4,3-c]quinoline (ELND006) and (*R*)-4-cyclopropyl-8-fluoro-5-(6-(trifluoromethyl)pyridin-3-ylsulfonyl)-4,5-dihydro-2*H*-pyrazolo[4,3-c]quinoline (ELND007): Metabolically stable gamma-secretase inhibitors that selectively inhibit the production of amyloid-beta over Notch. J Med Chem 56:5261–5274.
26. Oddo S, Caccamo A, Shepherd JD, Murphy G, Golde TE, Kayed R, *et al.* (2003): Triple-transgenic model of Alzheimer's disease with plaques and tangles: Intracellular Aβ and synaptic dysfunction. Neuron 39:409–421.
27. Lauritzen I, Pardossi-Piquard R, Bourgeois A, Pagnotta S, Biferi MG, Barkats M, *et al.* (2016): Intraneuronal aggregation of the β-CTF fragment of APP (C99) induces Aβ-independent lysosomal-autophagic pathology. Acta Neuropathol 132:257–276.
28. Sevalle J, Amoyel A, Robert P, Fournie-Zaluski MC, Roques B, Checler F (2009): Aminopeptidase A contributes to the N-terminal truncation of amyloid beta-peptide. J Neurochem 109:248–256.
29. Benkhelifa-Ziyyat S, Besse A, Roda M, Duque S, Astord S, Carcenac R, *et al.* (2013): Intramuscular scAAV9-SMN injection mediates widespread gene delivery to the spinal cord and decreases disease severity in SMA mice. Mol Ther 21:282–290.
30. Alves da Costa C, Paitel E, Mattson MP, Amson R, Telerman A, Ancolio K, *et al.* (2002): Wild-type and mutated presenilins 2 trigger p53-dependent apoptosis and down-regulate presenilin 1 expression in HEK293 human cells and in murine neurons. Proc Natl Acad Sci U S A 99:4043–4048.
31. Checler F (1999): Presenilins: Multifunctional proteins involved in Alzheimer's disease pathology. IUBMB Life 48:33–39.
32. Wolfe MS, Xia W, Ostaszewski BL, Diehl TS, Kimberly WT, Selkoe DJ (1999): Two transmembrane aspartates in presenilin-1 required for presenilin endoproteolysis and gamma-secretase activity. Nature 398:513–517.
33. Wolfe MS, Citron M, Diehl TS, Xia W, Donkor IO, Selkoe DJ (1998): A substrate-based difluoro ketone selectively inhibits Alzheimer's gamma-secretase activity. J Med Chem 41:6–9.
34. Lauritzen I, Pardossi-Piquard R, Bauer C, Brigham E, Abraham JD, Ranaldi S, *et al.* (2012): The β-secretase-derived C-terminal fragment

of βAPP, C99, but not Aβ, is a key contributor to early intraneuronal lesions in triple-transgenic mouse hippocampus. J Neurosci 32: 16243–16255a.

35. Bailey JA, Maloney B, Ge YW, Lahiri DK (2011): Functional activity of the novel Alzheimer's amyloid β-peptide interacting domain (AβID) in the APP and BACE1 promoter sequences and implications in activating apoptotic genes and in amyloidogenesis. Gene 488:13–22.
36. Maloney B, Lahiri DK (2011): The Alzheimer's amyloid β-peptide (Aβ) binds a specific DNA Aβ-interacting domain (AβID) in the *APP, BACE1*, and *APOE* promoters in a sequence-specific manner: Characterizing a new regulatory motif. Gene 488:1–12.
37. Ohyagi Y, Asahara H, Chui DH, Tsuruta Y, Sakae N, Miyoshi K, *et al.* (2005): Intracellular Abeta42 activates p53 promoter: A pathway to neurodegeneration in Alzheimer's disease. FASEB J 19:255–257.
38. Flammang B, Pardossi-Piquard R, Sevalle J, Debayle D, Dabert-Gay AS, Thevenet A, *et al.* (2012): Evidence that the amyloid-β protein precursor intracellular domain, AICD, derives from β-secretase-generated C-terminal fragment. J Alzheimers Dis 30:145–153.
39. Goodger ZV, Rajendran L, Trutzel A, Kohli BM, Nitsch RM, Konietzko U (2009): Nuclear signaling by the APP intracellular domain occurs predominantly through the amyloidogenic processing pathway. J Cell Sci 122:3703–3714.
40. Belyaev ND, Kellett KA, Beckett C, Makova NZ, Revett TJ, Nalivaeva NN, *et al.* (2010): The transcriptionally active amyloid precursor protein (APP) intracellular domain is preferentially produced from the 695 isoform of APP in a β-secretase-dependent pathway. J Biol Chem 285:41443–41454.
41. Lefranc-Jullien S, Sunyach C, Checler F (2006): APPepsilon, the epsilon-secretase-derived N-terminal product of the beta-amyloid precursor protein, behaves as a type I protein and undergoes alpha-, beta-, and gamma-secretase cleavages. J Neurochem 97:807–817.
42. Mei Y, Zhang Y, Yamamoto K, Xie W, Mak TW, You H (2009): FOXO3a-dependent regulation of Pink1 (Park6) mediates survival signaling in response to cytokine deprivation. Proc Natl Acad Sci U S A 106: 5153–5158.
43. Wang X, Wang Z, Chen Y, Huang X, Hu Y, Zhang R, *et al.* (2014): FoxO mediates APP-induced AICD-dependent cell death. Cell Death Dis 5:e1233.
44. Shimura H, Hattori N, Kubo S, Mizuno Y, Asakawa S, Minoshima S, *et al.* (2000): Familial Parkinson disease gene product, parkin, is a ubiquitin-protein ligase. Nat Genet 25:302–305.
45. da Costa CA, Sunyach C, Giaime E, West A, Corti O, Brice A, *et al.* (2009): Transcriptional repression of p53 by parkin and impairment by mutations associated with autosomal recessive juvenile Parkinson's disease. Nat Cell Biol 11:1370–1375.
46. Narendra DP, Jin SM, Tanaka A, Suen DF, Gautier CA, Shen J, *et al.* (2010): PINK1 is selectively stabilized on impaired mitochondria to activate parkin. PLoS Biol 8:e1000298.
47. Scarffe LA, Stevens DA, Dawson VL, Dawson TM (2014): Parkin and PINK1: Much more than mitophagy. Trends Neurosci 37:315–324.
48. Morais VA, Haddad D, Craessaerts K, De Bock PJ, Swerts J, Vilain S, *et al.* (2014): PINK1 loss-of-function mutations affect mitochondrial complex I activity via NdufA10 ubiquinone uncoupling. Science 344:203–207.
49. Vives-Bauza C, Zhou C, Huang Y, Cui M, de Vries RL, Kim J, *et al.* (2010): PINK1-dependent recruitment of parkin to mitochondria in mitophagy. Proc Natl Acad Sci U S A 107:378–383.
50. Narendra D, Tanaka A, Suen DF, Youle RJ (2008): Parkin is recruited selectively to impaired mitochondria and promotes their autophagy. J Cell Biol 183:795–803.
51. Mammucari C, Milan G, Romanello V, Masiero E, Rudolf R, Del Piccolo P, *et al.* (2007): FoxO3 controls autophagy in skeletal muscle in vivo. Cell Metab 6:458–471.
52. Webb AE, Brunet A (2014): FOXO transcription factors: Key regulators of cellular quality control. Trends Biochem Sci 39:159–169.
53. Klionsky DJ, Abdelmohsen K, Abe A, Abedin MJ, Abeliovich H, Acevedo Arozena A, *et al.* (2016): Guidelines for the use and interpretation of assays for monitoring autophagy (3rd edition). Autophagy 12:1–222.
54. Zhu Y, Chen G, Chen L, Zhang W, Feng D, Liu L, *et al.* (2014): Monitoring mitophagy in mammalian cells. Methods Enzymol 547:39–55.
55. Gegg ME, Cooper JM, Chau KY, Rojo M, Schapira AH, Taanman JW (2010): Mitofusin 1 and mitofusin 2 are ubiquitinated in a PINK1/parkin-dependent manner upon induction of mitophagy. Hum Mol Genet 19:4861–4870.
56. Wang H, Song P, Du L, Tian W, Yue W, Liu M, *et al.* (2011): Parkin ubiquitinates Drp1 for proteasome-dependent degradation: Implication of dysregulated mitochondrial dynamics in Parkinson disease. J Biol Chem 286:11649–11658.
57. Ghosal K, Vogt DL, Liang M, Shen Y, Lamb BT, Pimplikar SW (2009): Alzheimer's disease-like pathological features in transgenic mice expressing the APP intracellular domain. Proc Natl Acad Sci U S A 106:18367–18372.
58. Ryan KA, Pimplikar SW (2005): Activation of GSK3 and phosphorylation of CRMP2 in transgenic mice expressing APP intracellular domain. J Cell Biol 171:327–335.
59. Pardossi-Piquard R, Dunys J, Kawarai T, Sunyach C, Alves da Costa C, Vincent B, *et al.* (2007): Response to correspondence: Pardossi-Piquard et al., "Presenilin-dependent transcriptional control of the Abeta-degrading enzyme neprilysin by intracellular domains of betaAPP and APLP." Neuron 46, 541–554. Neuron 53:483–486.
60. Ross CA, Poirier MA (2004): Protein aggregation and neurodegenerative disease. Nat Med 10(suppl):S10–S17.
61. Takalo M, Salminen A, Soininen H, Hiltunen M, Haapasalo A (2013): Protein aggregation and degradation mechanisms in neurodegenerative diseases. Am J Neurodegener Dis 2:1–14.
62. Jucker M, Walker LC (2013): Self-propagation of pathogenic protein aggregates in neurodegenerative diseases. Nature 501:45–51.
63. Ciechanover A, Kwon YT (2015): Degradation of misfolded proteins in neurodegenerative diseases: Therapeutic targets and strategies. Exp Mol Med 47:e147.
64. Cai Y, Arikkath J, Yang L, Guo ML, Periyasamy P, Buch S (2016): Interplay of endoplasmic reticulum stress and autophagy in neurodegenerative disorders. Autophagy 12:225–244.
65. Nixon RA, Wegiel J, Kumar A, Yu WH, Peterhoff C, Cataldo A, *et al.* (2005): Extensive involvement of autophagy in Alzheimer disease: An immuno-electron microscopy study. J Neuropathol Exp Neurol 64:113–122.
66. Poole AC, Thomas RE, Andrews LA, McBride HM, Whitworth AJ, Pallanck LJ (2008): The PINK1/parkin pathway regulates mitochondrial morphology. Proc Natl Acad Sci U S A 105:1638–1643.
67. Wilhelmus MM, Nijland PG, Drukarch B, de Vries HE, van Horssen J (2012): Involvement and interplay of parkin, PINK1, and DJ1 in neurodegenerative and neuroinflammatory disorders. Free Radic Biol Med 53:983–992.
68. Beckett C, Nalivaeva NN, Belyaev ND, Turner AJ (2011): Nuclear signalling by membrane protein intracellular domains: The AICD enigma. Cell Signal 24:402–409.
69. Maloney B, Lahiri DK (2016): Epigenetics of dementia: Understanding the disease as a transformation rather than a state. Lancet Neurol 15:760–774.
70. Tatar M, Sedivy JM (2016): Mitochondria: Masters of epigenetics. Cell 165:1052–1054.
71. Robinson A, Grosgen S, Mett J, Zimmer VC, Haupenthal VJ, Hundsdorfer B, *et al.* (2014): Upregulation of PGC-1α expression by Alzheimer's disease-associated pathway: Presenilin 1/amyloid precursor protein (APP)/intracellular domain of APP. Aging Cell 13: 263–272.
72. Choi J, Ravipati A, Nimmagadda V, Schubert M, Castellani RJ, Russell JW (2014): Potential roles of PINK1 for increased PGC-1α-mediated mitochondrial fatty acid oxidation and their associations with Alzheimer disease and diabetes. Mitochondrion 18:41–48.
73. Cook DG, Leverenz JB, McMillan PJ, Kulstad JJ, Ericksen S, Roth RA, *et al.* (2003): Reduced hippocampal insulin-degrading enzyme in late-onset Alzheimer's disease is associated with the apolipoprotein E-e4 allele. Am J Pathol 162:313–319.
74. Checler F (1995): Processing of the β-amyloid precursor protein and its regulation in Alzheimer's disease. J Neurochem 65:1431–1444.